Stochastic Versus Deterministic Variability in Simple Neuronal Circuits: II. Hippocampal Slice

Steven J. Schiff,* Kristin Jerger,* Taeun Chang,* Tim Sauer,‡ and Peter G. Aitken§

*Department of Neurosurgery, Children's National Medical Center, Washington, D.C. 20010; ‡Department of Mathematics, George Mason University, Fairfax, Virginia 22030; and §Department of Cell Biology, Duke University Medical Center, Durham, North Carolina 27710 USA

ABSTRACT Long time series of Schaffer collateral to CA1 pyramidal cell presynaptic volleys (stratum radiatum) and population spikes (stratum pyramidale) were evoked (driven) in rat hippocampal slices. From the driven CA1 region in normal [K^+] perfusate, both population spike amplitude and an input-output function consisting of population spike amplitude divided by the presynaptic volley amplitude were analyzed. Raising [K^+] in the perfusion medium to 8.5 mM, slices were induced to spontaneously burst fire in CA3 and long time series of inter-burst intervals were recorded. Three tests for determinism were applied to these series: a discrete adaptation of a local flow approach, a local dispersion approach, and nonlinear prediction. Surrogate data were generated to serve as mathematical and statistical controls. All of the population spike (6/6) and input-output (6/6) time series from the normal [K^+] driven circuitry were stochastic by all three methods. Although most of the time series (5/6) from the autonomously bursting high [K^+] state failed to demonstrate evidence of determinism, one (1/6) of these time series did demonstrate significant determinism. This single instance of predictability could not be accounted for by the linear correlation in these data.

INTRODUCTION

In the preceding paper, we examined monosynaptic spinal cord reflex variability for evidence of determinism. It was noted that in the spinalized state, when the reflex circuitry is fairly well isolated from the rest of the nervous system, the variability in monosynaptic reflex amplitude is stochastic. This reflex amplitude is a measurement of the integrated area of the electrical potential recorded from a ventral root, and reflects the number of motoneurons discharging within the motoneuron pool (Rall, 1955). When the neural network connected to this reflex circuit is larger, in the decerebrate state, determinism can be observed. This predictability could not be accounted for by the linear correlation present in the decerebrate time series. To control for linear correlation in the experimental data, and provide a statistical null hypothesis that a linear stochastic system could account for our findings, we employed the method of surrogate data (for review, see Theiler et al., 1992), analyzing multiple sets of specially randomized data based on characteristics of the experimental data we wished to control for.

The spinal cord monosynaptic reflex shares a loosely analogous anatomy with certain regions of the brain, where sets of homogeneous afferents synapse on different sets of homogenous efferents, with recurrent efferent collateral fibers synapsing on inhibitory interneurons that feed back on the efferent neurons (Brodal, 1981). In regions of the brain such as the CA1 region of the hippocampus, population responses similar to monosynaptic reflexes can be measured in response to afferent impulses; as in the spinal cord monosynaptic reflex, the amplitude of such population responses appears to be proportional to the number of discharging cells (Andersen et al., 1971). Although such population recordings are customarily averaged to remove the variability inherent in such responses (Schiff and Somjen, 1985, 1987), we here examine the unaveraged responses for evidence of determinism.

In the CA1 region of the hippocampal slice, measurements from both the afferent presynaptic volley in the stratum radiatum and the efferent postsynaptic response in the stratum pyramidale can be recorded in response to stimulation of the afferent CA3 Schaffer collateral fibers. In our analysis, we will analyze both the population spike amplitudes, and the amplitude of an *input-output* transfer function created by dividing the population spike amplitude by the corresponding presynaptic volley amplitude.

Although in physiologic [K^+] CA1 pyramidal cells are generally quiescent unless driven with a stimulus, in high [K^+] this region exhibits spontaneous burst firing and electrographic seizure-like activity (Traynelis and Dingledine, 1988). This burst firing is driven from CA3, where the pyramidal cells autonomously burst fire without exhibiting electrographic seizure-like activity (Rutecki et al., 1985). This phenomenon in CA3 has been the subject of extensive investigations (Korn et al., 1987; Chamberlin et al., 1988–1990), and a detailed (and deterministic) mathematical model has been created that impressively replicates this behavior (Traub et al., 1990, 1991). We have induced spontaneous burst firing in CA3 with high [K^+], and we have created long time series by measuring the inter-burst intervals.

Three independent methods were used to test for the presence of determinism in these data. Again, the method of surrogate data was employed to control for the effects of linear correlation and provide a null hypothesis that the series

Received for publication 2 March 1994 and in final form 28 April 1994.

Address reprint requests to Steven J. Schiff, M.D., Ph.D., Department of Neurosurgery, Children's National Medical Center, 111 Michigan Avenue, N.W., Washington, D.C. 20010. Tel.: 202-884-3020; Fax: 202-884-3091.

0006-3495/94/08/684/08 $2.00

of intervals observed could be accounted for by the activity of a stochastic linear system.

Portions of this work have appeared in abstract form (Aitken et al., 1993).

MATERIALS AND METHODS

Female Sprague-Dawley rats weighing 125–150 g were anesthetized with diethyl-ether and decapitated. Transverse slices of 400 μm were prepared with a tissue chopper and placed in an interface type perfusion chamber at 32–35°C. Slices were perfused with artificial cerebrospinal fluid (ACSF) composed of 155 mM Na^+, 136 mM Cl^-, 3.5 mM K^+, 1.2 mM Ca^{2+}, 1.2 mM Mg^{2+}, 1.25 mM $(PO_4)^{2-}$, 24 mM $(HCO_3)^-$, 1.2 mM $(SO_4)^{2-}$, and 10 mM dextrose, flowing at 2 ml/min. After 90 min of incubation, slices were tested for viability by recording a greater than 2 mV unitary population spike in the stratum pyramidale of CA1, in response to stimulation of Schaffer collateral fibers in the CA1 stratum radiatum with 100 μs constant current 50–150 μA square-wave pulses delivered at 0.1 Hz through tungsten microelectrodes. Recordings were made with 2–4 MΩ glass needle electrodes filled with 150 mM NaCl. With confirmation of viability, one of the following two experimental procedures were performed.

The first experimental paradigm consisted of recording a series of evoked population spikes in the stratum pyramidale and presynaptic volleys in the stratum radiatum of CA1, in response to just submaximal stimulation delivered to the Schaffer collateral fibers at 0.1 Hz. Data were digitized across 12 bits at 5 KHz with a Digidata 1200 analog to digital converter (Axon Instruments, Foster City, CA) and stored on a personal computer using Axotape 2.0 (Axon Instruments). Population spike and presynaptic volley peak to peak amplitudes were measured with Datapac II (Run Technologies, Laguna Hills, CA) as illustrated in Fig. 1, *A* and *B*.

We analyzed both the raw population spike amplitudes and created an input-output function consisting of population spike divided by presynaptic volley amplitude. Because of this, the population spike and input-output data each reflected six data sets from six experiments and are not statistically independent. Because population spike amplitudes could demonstrate marked linear drift over the course of an experiment, the population spike and input-output time series had any linear trend removed (first order-detrended) using Statgraphics 6.0 (Manugistics, Rockville, MD).

The second experimental paradigm consisted of switching the perfusate to ACSF containing 8.5 mM $[K^+]$ and 141 mM $[Cl^-]$, the rest of the ionic concentrations unchanged from those given above. After 15–20 min of high $[K^+]$ perfusion, spontaneous burst firing could be recorded from CA3a or CA3b. Simultaneous recordings from the stratum pyramidale were made in CA1, but these CA1 data will not be reported here. Recordings were digitized as above, and CA3 interburst intervals were measured with Datapac II (Run Technologies) as illustrated in Fig. 1 *C*. No detrending for these data was required.

Three independent tests for determinism were used: local flow, local dispersion, and nonlinear prediction. Background theory for these methods is explained in the preceding paper in detail, where an Appendix contains the mathematics. Surrogate data methods and autocorrelation are similarly discussed in detail in the preceding paper.

RESULTS

Normal $[K^+]$-driven system

Six time series were collected from six experiments. Fig. 2 shows the original experimental time series of the population spike amplitudes (PS) along with the time series of calculated input-output amplitudes (IO).

Fig. 3 shows the autocorrelation of the original time series and input-output values. Although significant linear correlation was observed for these series, no oscillations were observed, in contrast to the decerebrate spinal cord monosynaptic reflexes in the preceding paper. These long nonoscillatory correlations in time are in part caused by experimental drift in the excitability of this in vitro system.

To validate the determinism algorithms we used (local flow, local dispersion, and nonlinear prediction), we have tested them with a chaotic time series generated from deterministic equations, and these results are illustrated for the Hénon equations in the preceding paper. For each time series, three independent realizations of each of three types of

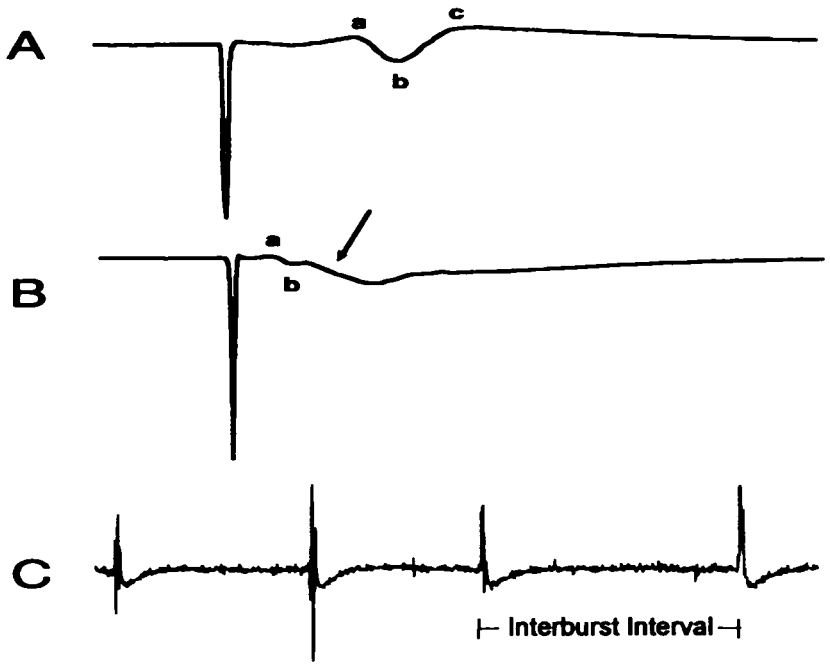

FIGURE 1 (*A*) Examples of evoked population spikes recorded in stratum pyramidale of CA1 in response to CA3 Schaffer collateral fiber stimulation. Amplitude calculated by averaging the potential at the two maxima a and c, and subtracting the potential at minimum b. (*B*) Evoked presynaptic volley in stratum radiatum of CA1, recorded simultaneously with trace in *A*. Amplitude calculated as difference between maximum a and minimum b. Arrow points to region where the rate of change of potential (maximal slope) reflects the magnitude of the field excitatory postsynaptic potential. An *input-output* function was calculated by dividing each population spike by its corresponding presynaptic volley. (*C*) Spontaneous burst firing in CA3 in high $[K^+]$. Interburst intervals calculated as shown. For all of the above calculations, the interburst intervals identified with Datapac II (Run Technologies) were verified visually throughout each data set to ensure accuracy.

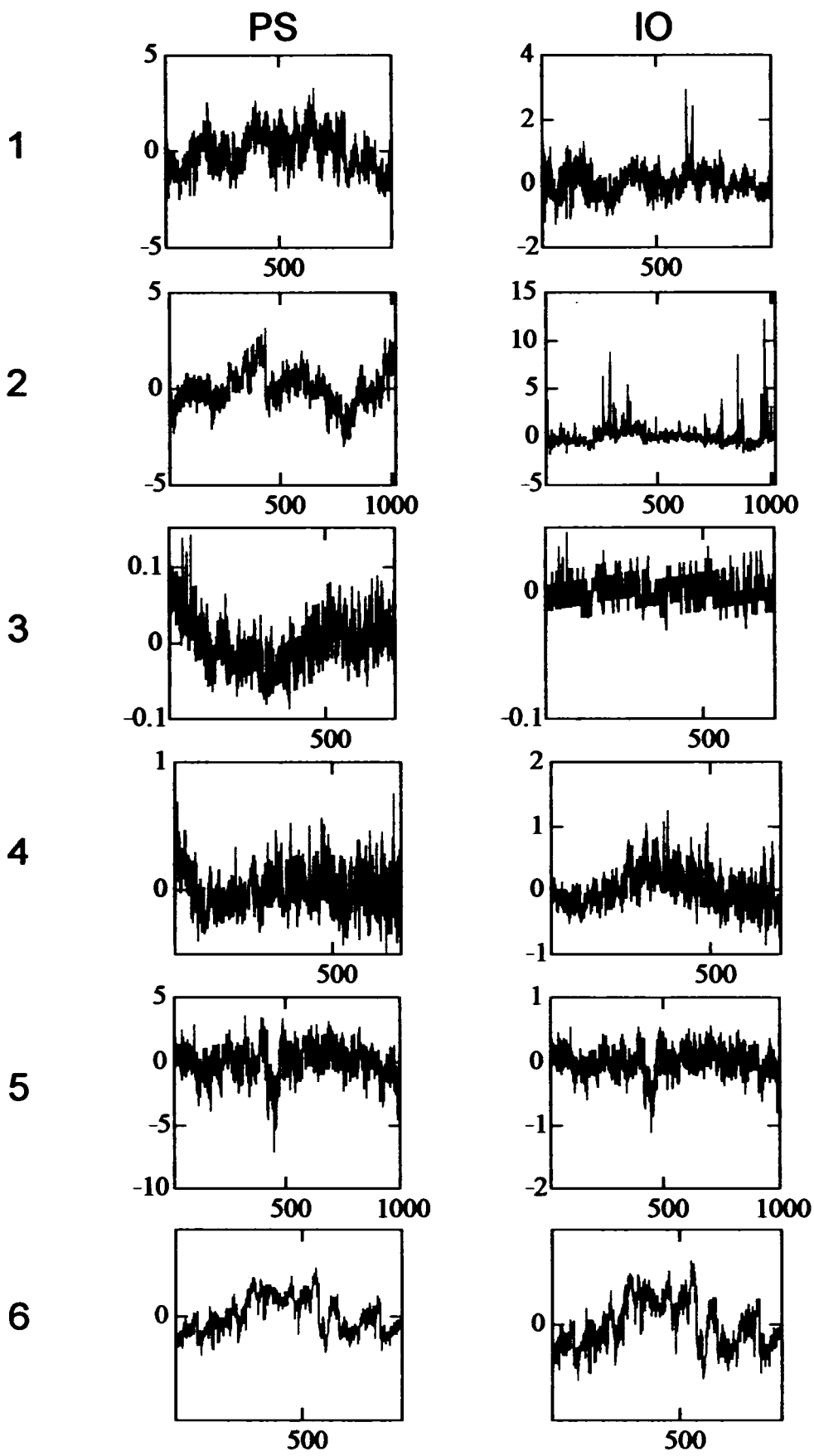

FIGURE 2 Population spike (PS) time series and input-output (IO) time series for evoked data in normal [K^+]. Input-output series calculated by dividing each efferent population spike by its corresponding afferent presynaptic volley. These time series were first order-detrended (linear trend-removed) to compensate for the drift in amplitudes observed for this type of experiment.

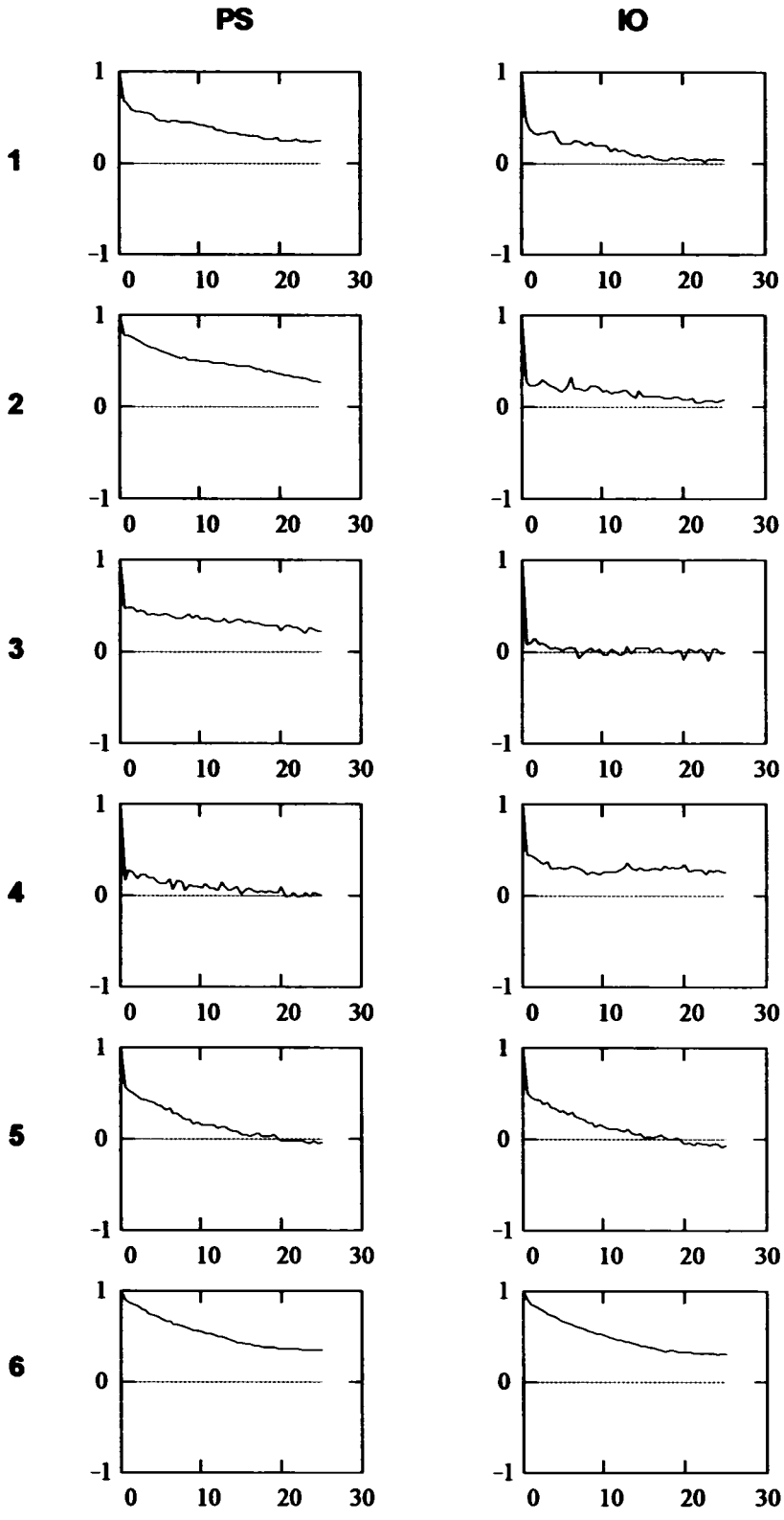

FIGURE 3 Autocorrelation for population spike (PS) and input-output (IO) time series. Abscissa are time lags in s.

surrogate data (with different random numbers) were generated. We focus on the least separation between surrogate and experimental results, because if any surrogate data can fit the results well, determinism is not likely present. To quantify these results, we used a technique suggested by Theiler et al. (1992), where for each point plotted along the abscissa, the SD is calculated for the surrogate data, and the number of SDs separating the surrogate mean from the experimental values, "sigmas," are determined.

All of the population spike time series (6/6) and all of the input-output time series (6/6) failed to demonstrate evidence

of determinism. Much caution was called for to avoid spurious conclusions here. Fig. 4 shows an example of a stochastic result from an input-output time series for experiment 2 (Fig. 2, IO). Note the separation between data analyzed with nonlinear prediction and the surrogate data. The experimental results and surrogate data results were separated by an average of about 2 SDs for the first five translation horizons. However, the values of normalized prediction error are greater than 1.0, indicating that our prediction errors were actually *worse* than choosing the mean of the time series as a prediction. This is not a demonstration of nonlinear determinism.

For the high [K^+] experiments, the interval series are shown in Fig. 5. Autocorrelation for these data are shown in Fig. 6, and there is little linear correlation evident in any of these series.

Only one (1/6) spontaneously bursting high [K^+] experimental time series showed evidence for determinism, and only with nonlinear prediction. The results of local flow, local dispersion, and nonlinear prediction for this time series (experiment 5, Fig. 5) are shown in Fig. 7. The closest surrogate fit for Fourier-shuffled surrogates averaged 8.1 sigmas below the surrogate data mean for the first four translation horizons, and it appeared significant.

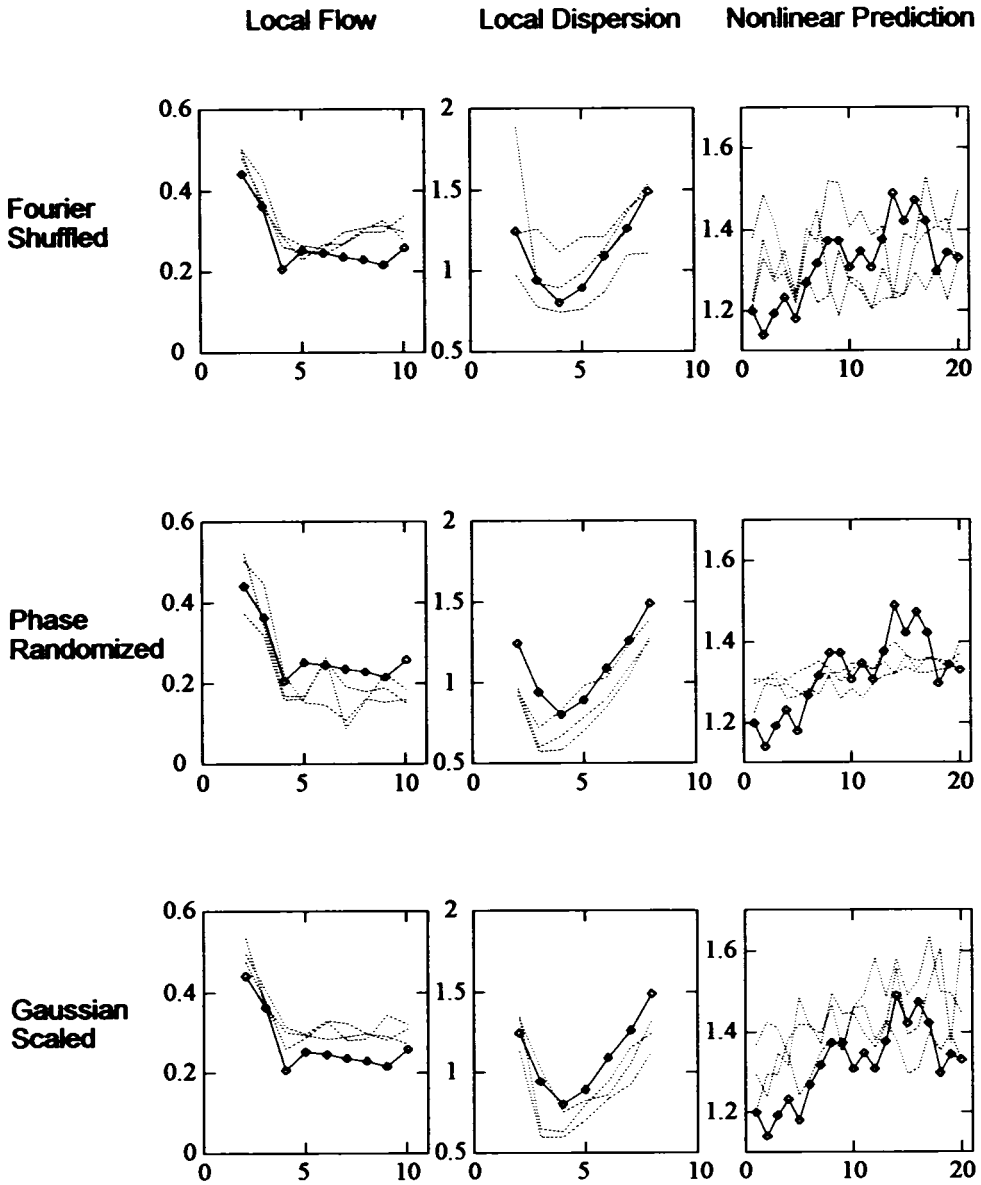

FIGURE 4 Results of local flow, local dispersion, and nonlinear prediction algorithms on data from the input-output time series from experiment 2 (Fig. 2). Each method of analysis compares the results from the experimental data with three sets of each of the three types of surrogate data. Diamonds (◇) represent experimental results, and dashed lines (- - - -) represent surrogate data results, in this and subsequent figures. This is a stochastic result, even for nonlinear prediction, where the prediction errors are less than the surrogate data errors. Note, however, that the absolute values of the normalized prediction errors are greater than 1.0, indicating that the algorithm was worse than a prediction based on guessing the mean of the time series. Caution must be exercised in the application of these algorithms, especially when the numbers of SDs separating experimental from surrogate data results are small, (e.g., 2 or 3). The abscissa are translation horizon for local flow and nonlinear prediction, and embedding dimension for local dispersion plots. Embedding dimensions are 4 and 8 for local flow and nonlinear prediction, respectively, and local dispersion translation horizons are 1 in this and subsequent plots.

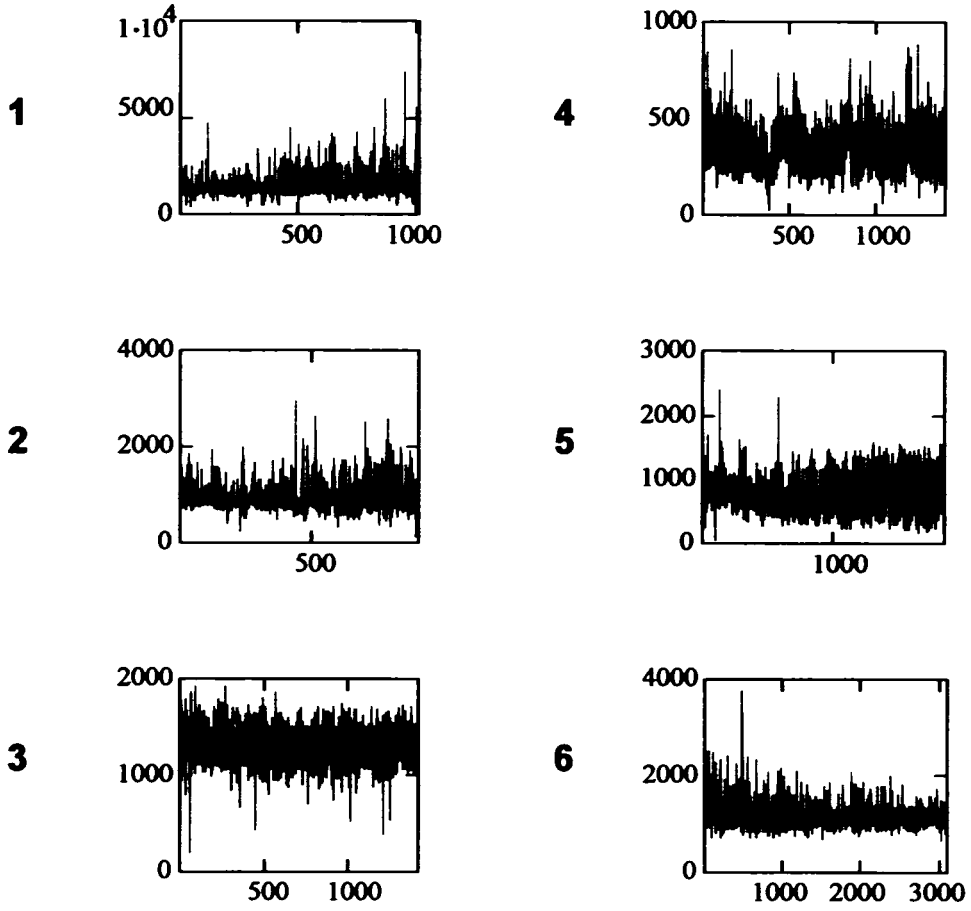

FIGURE 5 Interburst interval data in high $[K^+]$. The ordinates are time in ms, and the abscissa are event numbers.

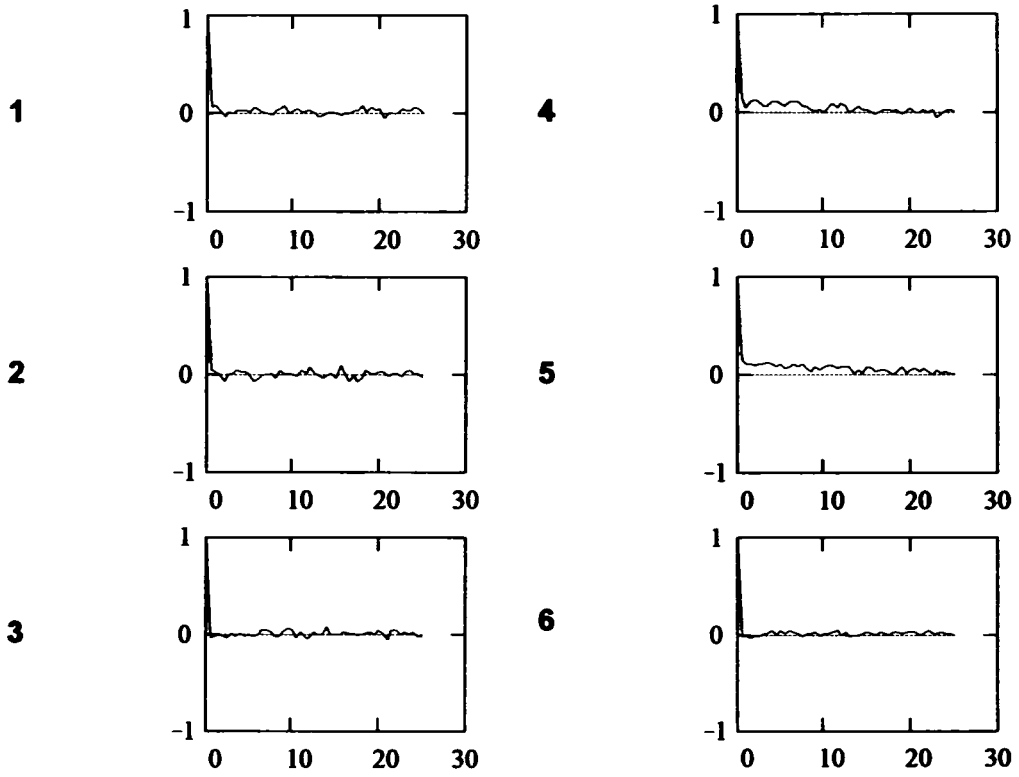

FIGURE 6 Autocorrelation for interburst interval data in Fig. 6. Little, if any, linear correlation is demonstrated for any of these data. The spectral characteristics of such data resemble those of white noise.

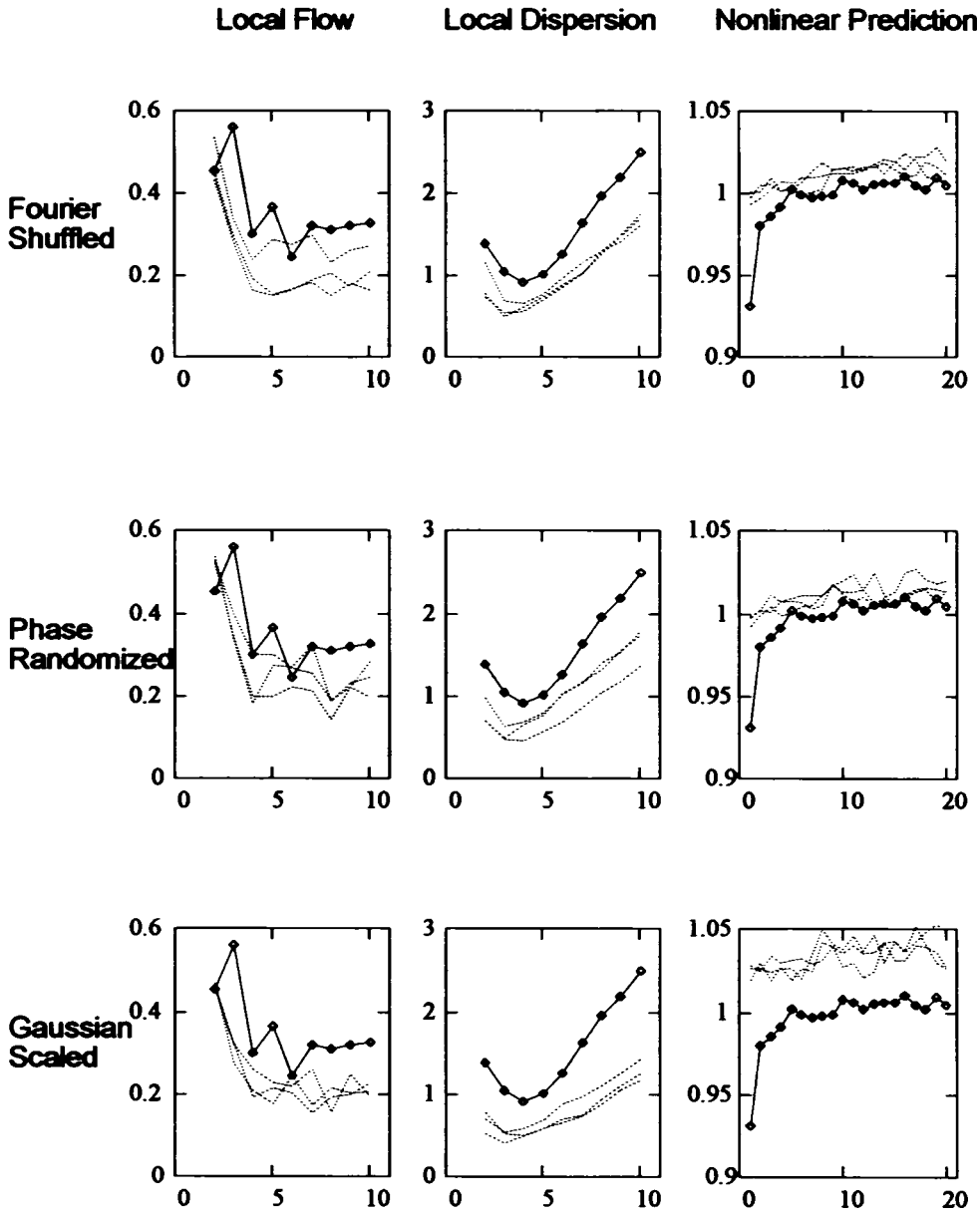

FIGURE 7 Results of local flow, local dispersion, and nonlinear prediction algorithms on data from the input-output time series from experiment 5 (Fig. 5). This is a deterministic result for nonlinear prediction, and these results are quantified in the text.

DISCUSSION

Without exception (12/12), the population spike and input-output time series failed to demonstrate deterministic structure. This isolated monosynaptic population response, similar to the spinalized monosynaptic spinal cord reflex, behaves stochastically.

With one exception (1/6), spontaneous burst firing in CA3 in high $[K^+]$ appeared stochastic (5/6). In the one example of deterministic structure from these time series, the statistical confidence that determinism was present was significant. To our knowledge, the preparation of these experiments was similar, and we can offer no explanation for the solitary deterministic finding.

From both spinal cord and brain, responses involving larger scale neuronal network behavior seem more capable of demonstrating determinism than the responses from more isolated circuitry. The experiment we did not perform here, comparing driven population responses in CA1 as a function of normal versus high $[K^+]$, would serve as an intriguing analogy to the spinal cord experiments.

We were concerned that the long autocorrelation found in the driven slice data in normal $[K^+]$ could lead to spurious results because of the long coherence times themselves (Theiler et al., 1993). Fortunately, we observed no such effects for normal $[K^+]$ data that our surrogate data did not account for. The only deterministic result was for an autonomously bursting slice in high $[K^+]$, and none of these data demonstrated substantial linear correlation.

There is a theoretical issue for the spontaneous burst firing data that is incompletely addressed at present. The three methods used to detect determinism, local flow (Kaplan, 1993), local dispersion (Wayland et al., 1993), and nonlinear prediction (Sugihara and May, 1990), have been developed for time series data where an observable quantity is measured

at fixed intervals of time. There is little theoretical study regarding whether such methods are equally effective when applied to time interval data, where each measurement in the series constitutes an event number rather than a discrete interval of time. A more effective methodology for detecting predictability in such interval data might reveal more prevalent determinism than we have found so far. Nevertheless, recent work suggests that reconstruction of dynamics from interval data can be as valid as from time series (Sauer, 1994).

If information is processed in the brain using small populations of neurons as studied here (a statement of mere conjecture at this point), then it is critical to understand whether such circuits process information stochastically or deterministically. In addition, if control must be imposed on such circuitry, the control method used must take into account the degree of predictability (or lack thereof) of the system. Whether elements of the nervous system employ some degree of control over neighboring elements with strategies based on predictability, or whether such circuitry can be controlled externally with sophisticated consideration of nonlinear deterministic structure (Ott et al., 1990; Shinbrot et al., 1993), are now technologically tractable questions. Further work will demonstrate whether such control strategies have any applicability for the simple neuronal systems studied here (S. J. Schiff, K. Jerger, D. H. Duong, T. Chang, M. L. Spano, and W. L. Ditto, unpublished data).

Portions of this work were supported by a grant to S. J. Schiff from National Institutes of Health (1 R29 MH50006-01), and support from the Children's Research Institute. T. Chang receives support from the Children's Research Institute. T. Sauer is partially supported by the National Science Foundation Computational Mathematics program and the Department of Energy. The contribution of software from Manugistics, Inc. is greatly appreciated.

REFERENCES

Aitken, P. G., T. Sauer, and S. J. Schiff. 1993. Stochastic versus deterministic variability in hippocampal CA1 population spikes. *Soc. Neurosci. Abstr.* 19:1598.

Andersen, P., T. V. P. Bliss, and K. K. Skrede. 1971. Unit analysis of hippocampal population spikes. *Exp. Brain. Res.* 13:208–221.

Brodal, A. 1981. Neurological Anatomy. New York. 1053 pp.

Chamberlin, N. L., and R. Dingledine. 1988. GABAergic inhibition and the induction of spontaneous epileptiform activity by low chloride and high potassium in the hippocampal slice. *Brain Res.* 445:12–18.

Chamberlin, N. L., and R. Dingledine. 1989. Control of epileptiform burst rate by CA3 hippocampal cell afterhyperpolarizations in vitro. *Brain Res.* 492:337–346.

Chamberlin, N. L., R. D. Traub, and R. Dingledine. 1990. Role of EPSPs in initiation of spontaneous synchronized burst firing in rat hippocampal neurons bathed in high potassium. *J. Neurophysiol.* 64:1000–1007.

Kaplan, D. T. 1993. Evaluating deterministic structure in maps deduced from discrete-time measurements. *Int. J. Bifurcations and Chaos.* In press.

Korn, S. J., J. L. Giacchino, N. L. Chamberlin, and R. Dingledine. 1987. Epileptiform burst activity induced by potassium inthe hippocampus and its regulation by GABA-mediated inhibition. *J. Neurophysiol.* 57: 325–340.

Ott, E., C. Grebogi, and J. A. Yorke. 1990. Controlling chaos. *Phys. Rev. Lett.* 64:1196–1199.

Rall, W. 1955. Experimental monosynaptic input-output relations in the mammalian spinal cord. *J. Cell Comp. Physiol.* 46:413–437.

Rutecki, P. A., F. J. Lebeda, and D. Johnson. 1985. Epileptiform activity induced by changes in extracellular potassium in hippocampus. *J. Neurophysiol.* 54:1363–1374.

Sauer, T. 1994. Reconstruction of dynamical systems from interspike intervals. *Phys. Rev. Lett.* 72:3811–3814.

Schiff, S. J., and T. Chang. 1992. Differentiation of linearly correlated noise from chaos in a biologic system using surrogate data. *Biol. Cybernet.* 67:387–393.

Schiff, S. J., and G. G. Somjen. 1985. The effects of temperature on synaptic transmission in hippocampal tissue slices. *Brain Res.* 345:279–284.

Schiff, S. J., and G. G. Somjen. 1987. The effect of graded hypoxia on the hippocampal slice: an in vitro model of the ischemic penumbra. *Stroke.* 18:30–37.

Shinbrot, T., C. Grebogi, E. Ott, and J. A. Yorke. 1993. Using small perturbations to control chaos. *Nature.* 363:411–417.

Sugihara, G., and R. M. May. 1990. Nonlinear forecasting as a way of distinguishing chaos from measurement error in time series. *Nature.* 344: 734–741.

Theiler, J., S. Eubank, A. Longtin, B. Galdrikian, and J. D. Farmer. 1992. Testing for nonlinearity in time series: the method of surrogate data. *Physica D.* 58:77–94.

Theiler, J., P. Linsay, and D. M. Rubin. 1993. Detecting nonlinearity in data with long coherence times. *In* Time Series Prediction: Forecasting the Future and Understanding the Past. A. S. Weigend and N. A. Gershenfeld (editors). SFI Studies in the Sciences of Complexity. Vol. 15. Addison-Wesley, Reading, MA. 430–455.

Traub, R. D., and R. Dingledine. 1990. Model of synchronized epileptiform bursts induced by high potassium in CA3 region of rat hippocampal slice. Role of spontaneous EPSPs in initiation. *J. Neurophysiol.* 64:1009–1017.

Traub, R. D., and R. Miles. 1991. Neuronal networks of the hippocampus. Cambridge University Press, Cambridge, England. 281 pp.

Traynelis, A. F., and R. Dingledine. 1988. Potassium-induced spontaneous electrographic seizures in the rat hippocampal slice. *J. Neurophysiol.* 59:259–276.

Wayland, R., D. Bromley, D. Pickett, and A. Passemante. 1993. Recognizing determinism in a time series. *Phys. Rev. Lett.* 70:580–582.